

QUIESCENT NUCLEAR BURNING IN LOW-METALLICITY WHITE DWARFS

MARCELO M. MILLER BERTOLAMI^{1,2,5,6}, LEANDRO G. ALTHAUS^{1,2}, AND ENRIQUE GARCÍA-BERRO^{3,4}

¹ Facultad de Ciencias Astronómicas y Geofísicas, Universidad Nacional de La Plata, Paseo del Bosque s/n, 1900 La Plata, Argentina

² Instituto de Astrofísica de La Plata, UNLP-CONICET, Paseo del Bosque s/n, 1900 La Plata, Argentina

³ Departament de Física Aplicada, Universitat Politècnica de Catalunya, c/Esteve Terrades 5, E-08860 Castelldefels, Spain

⁴ Institute for Space Studies of Catalonia, c/Gran Capita 2–4, Edif. Nexus 104, E-08034 Barcelona, Spain

Received 2013 July 19; accepted 2013 August 7; published 2013 September 6

ABSTRACT

We discuss the impact of residual nuclear burning in the cooling sequences of hydrogen-rich (DA) white dwarfs with very low metallicity progenitors ($Z = 0.0001$). These cooling sequences are appropriate for the study of very old stellar populations. The results presented here are the product of self-consistent, fully evolutionary calculations. Specifically, we follow the evolution of white dwarf progenitors from the zero-age main sequence through all the evolutionary phases, namely the core hydrogen-burning phase, the helium-burning phase, and the thermally pulsing asymptotic giant branch phase to the white dwarf stage. This is done for the most relevant range of main-sequence masses, covering the most usual interval of white dwarf masses—from $0.53 M_{\odot}$ to $0.83 M_{\odot}$. Due to the low metallicity of the progenitor stars, white dwarfs are born with thicker hydrogen envelopes, leading to more intense hydrogen burning shells as compared with their solar metallicity counterparts. We study the phase in which nuclear reactions are still important and find that nuclear energy sources play a key role during long periods of time, considerably increasing the cooling times from those predicted by standard white dwarf models. In particular, we find that for this metallicity and for white dwarf masses smaller than about $0.6 M_{\odot}$, nuclear reactions are the main contributor to the stellar luminosity for luminosities as low as $\log(L/L_{\odot}) \simeq -3.2$. This, in turn, should have a noticeable impact in the white dwarf luminosity function of low-metallicity stellar populations.

Key words: stars: evolution – stars: interiors – white dwarfs

1. INTRODUCTION

White dwarf stars are the most common end-point of stellar evolution and as such are routinely used in constraining several properties of stellar populations including our Galaxy as a whole, as well as globular and open clusters—see, for instance, Hansen et al. (2007), Winget et al. (2009), García-Berro et al. (2010), and Bono et al. (2013), and references therein. In addition to these applications, white dwarfs have also been employed to test physics under conditions that cannot be attained in terrestrial laboratories. In particular, they have been used to place constraints on the properties of elementary particles such as axions—see Isern et al. (2008) and Córscico et al. (2012a, 2012b) for recent efforts—and neutrinos (Winget et al. 2004), or on alternative theories of gravitation (García-Berro et al. 1995, 2011; Córscico et al. 2013). The use of white dwarfs for all of these applications and as precise stellar chronometers requires a detailed knowledge of the main physical processes that control their evolution—see Fontaine & Brassard (2008), Winget & Kepler (2008), and Althaus et al. (2010b) for extensive reviews.

These and other potential applications of white dwarfs has led to renewed efforts in computing full evolutionary models for these stars, taking into account all the relevant sources and sinks of energy (Renedo et al. 2010; Salaris et al. 2010; Althaus et al. 2010c). However, in most calculations, stable nuclear burning is not considered. This assumption is well justified because stable hydrogen shell burning is expected to be a minor source of energy for stellar luminosities below $\sim 100 L_{\odot}$. Thus, in a typical white dwarf, H burning is not a relevant energy source as soon as the hot part of the white dwarf cooling track is reached.

Nevertheless, in regular white dwarfs H burning never ceases completely, and depending on the mass of the white dwarf and on the precise mass of H left during the previous evolutionary phases (which depends critically on metallicity), it may become a non-negligible energy source for white dwarfs with hydrogen atmospheres. Actually, a correct assessment of the role played by residual H burning during the cooling phase requires a detailed calculation of the white dwarf progenitor history. As a matter of fact, the full evolutionary calculations of Renedo et al. (2010) already showed that in white dwarfs resulting from progenitors with $Z = 0.001$ residual H burning via the proton–proton (*pp*) chains may contribute by about 30% to the luminosity by the time cooling has proceeded down to luminosities ranging from $L \sim 10^{-2} L_{\odot}$ to $10^{-3} L_{\odot}$. Nevertheless, the impact of nuclear burning on the cooling times has been found to be almost negligible in almost all the cases studied so far. However, it is worth noting that with the exception of a few sequences computed by Miller Bertolami et al. (2011), the only white dwarf cooling sequences derived from the consistent evolution of their low-metallicity progenitor stars computed up to now have been performed for metallicities $Z \geq 0.001$ (Renedo et al. 2010).

In this Letter, we show that stable H burning becomes the dominant energy source of white dwarfs resulting from very low-metallicity progenitors, namely with $Z \approx 0.0001$, delaying their cooling for significant time intervals. To arrive at this result, we have computed the full evolution of white dwarf stars taking into account the evolutionary history throughout all the evolutionary stages of their progenitor stars with $Z = 0.0001$. This is the metal content of some old stellar populations like the galactic halo or globular clusters. Thus, we are forced to conclude that standard white dwarf sequences that do not take into account the energy release of the H-burning shell are not appropriate for the study of such very low-metallicity populations.

⁵ Also at Max-Planck-Institut für Astrophysik, Karl-Schwarzschild Strasse 1, D-85748 Garching, Germany.

⁶ Post-doctoral Fellow of the Alexander von Humboldt Foundation.

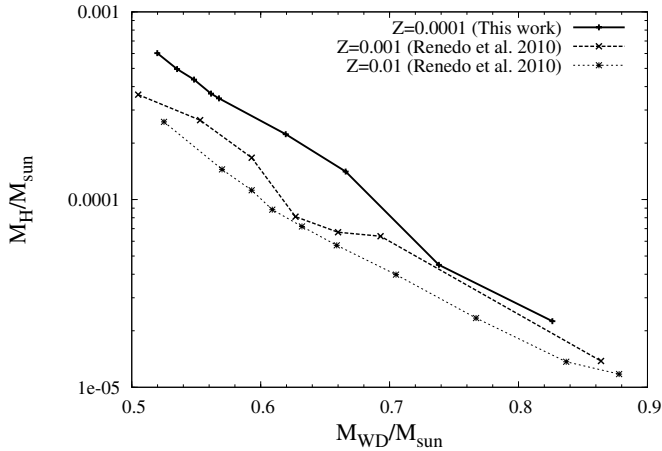


Figure 1. Total hydrogen content of the white dwarf models at the beginning of the cooling branch of the very low-metallicity models presented here ($Z = 0.0001$) as a function of the mass, compared with the hydrogen content of the models of higher metallicity computed by Renedo et al. (2010) for $Z = 0.001$ and $Z = 0.01$. Note the change in the slope due to the occurrence of the third dredge-up for the two more massive model sequences, which tends to reduce the size of the resulting H envelope.

2. EVOLUTIONARY CODE AND INPUT PHYSICS

The calculations reported here have been done using the LPCODE stellar evolutionary code (Althaus et al. 2012). This code has been used to study different problems related to the formation and evolution of white dwarfs (García-Berro et al. 2010; Althaus et al. 2010a; Renedo et al. 2010; Miller Bertolami et al. 2011). A description of the input physics and numerical procedures employed in LPCODE can be found in these works. In particular, convective overshooting has been considered during the core H and He burning, but not during the thermally pulsing asymptotic giant branch (TP-AGB). Mass loss during the red giant branch (RGB) and AGB phases has been considered following the prescriptions of Schröder & Cuntz (2005) and Groenewegen et al. (2009). The nuclear network accounts for 16 isotopes together with 34 thermonuclear reaction rates for the pp chains, CNO bi-cycle, helium burning, and carbon ignition that are identical to those described in Althaus et al. (2005), with the exception of the $^{12}\text{C} + p \rightarrow ^{13}\text{N} + \gamma \rightarrow ^{13}\text{C} + e^+ + \nu_e$, and $^{13}\text{C}(p,\gamma)^{14}\text{N}$ reaction rates, which are taken from Angulo et al. (1999). Radiative opacities are those of OPAL (Iglesias & Rogers 1996). Conductive opacities are from Cassisi et al. (2007). The screening factors adopted in this work are those of Graboske et al. (1973). The equation of state during the main-sequence evolution is that of the OPAL project for H- and He-rich compositions for the appropriate metallicity. Finally, updated low-temperature molecular opacities with varying carbon–oxygen ratios are used. To this end, we have adopted the low temperature opacities of Ferguson et al. (2005) and Weiss & Ferguson (2009). In LPCODE molecular opacities are computed adopting the opacity tables with the correct abundances of the unenhanced metals (e.g., Fe) and the appropriate carbon–oxygen ratio.

For the white dwarf regime, we take into account the effects of element diffusion due to gravitational settling, chemical and thermal diffusion; see Althaus et al. (2003) for details. For effective temperatures lower than 10,000 K, outer boundary conditions are derived from non-gray model atmospheres (Rohrman et al. 2012). Both latent heat release and the release of gravitational energy resulting from carbon–oxygen phase separation

Table 1
Characteristics of our Initial White Dwarf Models

$M_{\text{ZAMS}}/M_{\odot}$	M_{WD}/M_{\odot}	τ	M_{H}/M_{\odot}
0.80	0.51976	12.844	6.03×10^{-4}
0.85	0.53512	10.368	4.96×10^{-4}
0.90	0.54839	8.441	4.36×10^{-4}
0.95	0.56145	6.998	3.67×10^{-4}
1.00	0.56765	5.887	3.46×10^{-4}
1.25	0.61940	2.887	2.23×10^{-4}
1.50	0.66588	1.582	1.41×10^{-4}
2.00	0.73821	0.751	4.49×10^{-5}
2.50	0.82623	0.421	2.25×10^{-5}

(Isern et al. 2000, 1997) have been included following the phase diagram of Horowitz et al. (2010); see Althaus et al. (2012) for details of the numerical implementation. Finally, we emphasize that recently, LPCODE has been tested against other white dwarf evolutionary codes and uncertainties in the cooling ages arising from different numerical implementations of stellar evolution equations were found to be below 2% (Salaris et al. 2013).

It is worth commenting that for a correct assessment of the H content and of the residual nuclear burning on cool white dwarfs, the full calculation of the evolutionary stages leading to the formation of the white dwarf is absolutely necessary. This cannot be done using artificial initial white dwarf structures, since in this case the mass of the hydrogen envelope, which determines the importance of nuclear burning, is artificially imposed and then lacks predictive power. For this reason, we have followed the complete evolution of the progenitor stars computing all the evolutionary stages throughout the entire lifetime of the progenitor of the white dwarf, starting from the zero-age main sequence (ZAMS) and continuing through the rather computationally complex TP-AGB phase. In particular, we computed full nine white dwarf evolutionary sequences adopting for the progenitor stars $Z = 0.0001$ and an initial H mass fraction of $X_{\text{H}} = 0.7547$. We note that in our calculations we did not find any third dredge-up episode during the TP-AGB phase, except for the two more massive sequences, those with initial ZAMS masses 2.0 and $2.5 M_{\odot}$. This is due to the low initial stellar masses and metallicity, of the sequences computed in this work. In Table 1, we list the main results of our calculations. In particular, we list the initial mass of the progenitor stars at the ZAMS, the final mass of the resulting white dwarf—both in solar units—the progenitor lifetime (in Gyr), and the mass of H at the beginning of the cooling branch—that is, at the point of maximum effective temperature—in solar masses. As expected, the residual H content decreases with increasing white dwarf masses, a trend which helps to understand the dependence of residual nuclear burning on the stellar mass discussed in the next section. In all cases, the white dwarf evolution has been computed down to $\log(L/L_{\odot}) = -5.0$.

3. THE IMPACT OF NUCLEAR BURNING ON THE COOLING TIMES

As shown by Iben & MacDonald (1986), low-metallicity progenitors depart from the AGB with more massive envelopes, leading to white dwarfs with thicker H envelopes. This well-known behavior can be seen in Figure 1, where the total hydrogen content of the initial white dwarf models computed in the present work ($Z = 0.0001$) is compared with that of models with higher metallicity computed by Renedo et al. (2010), that

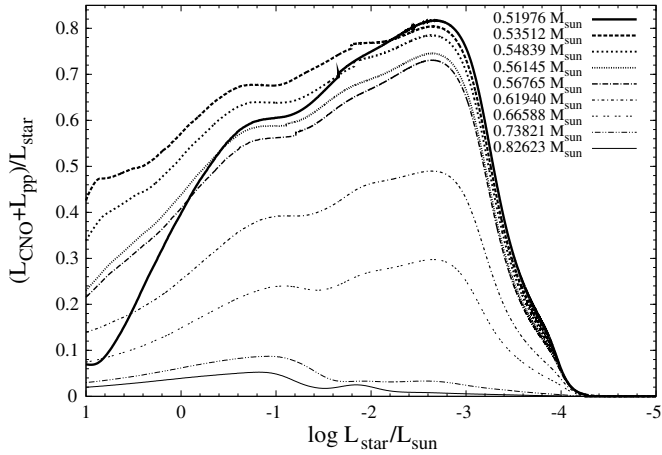


Figure 2. Fraction of the total luminosity due to nuclear burning for different white dwarf sequences with $Z = 0.0001$. Note that for white dwarf masses below $\sim 0.6 M_{\odot}$ nuclear burning becomes the main energy source of the white dwarf.

have somewhat larger metallicities ($Z = 0.001$ and $Z = 0.01$). As a result of the larger H envelopes, residual H burning is expected to become more relevant in white dwarfs with low-metallicity progenitors. In particular, our results show that, at the metallicity of the galactic halo and some old globular cluster ($Z \sim 0.0001$), stable H burning becomes one of the main energy sources of *low-mass* white dwarfs for substantial periods of time. This is better illustrated in Figure 2, where we show the fraction of the surface luminosity that is generated by nuclear burning at different stages of the white dwarf cooling phase. It is apparent that the luminosity of white dwarfs descending from metal-poor progenitors is completely dominated by nuclear burning, even at rather low luminosities. Specifically, note that for white dwarfs with $M \lesssim 0.6 M_{\odot}$ nuclear energy release constitutes the main energy source at intermediate luminosities ($-3.2 \lesssim \log(L/L_{\odot}) \lesssim -1$). This leads to a very significant delay in the cooling times, as compared with stars with solar metallicity in which nuclear burning does not play a leading role, and most of the energy release comes from the thermal energy stored in the interior. This is shown in Figure 3, which displays the different cooling curves (left panels) of selected low-metallicity white dwarf sequences when nuclear energy sources are considered or disregarded, and the corresponding delays introduced by nuclear burning (right panels). It is quite apparent that neglecting the energy released by nuclear burning leads to an underestimation of the cooling times by more than a factor of two at intermediate luminosities. This is true for white dwarfs resulting from low-metallicity progenitors with $M_{\text{WD}} \lesssim 0.6 M_{\odot}$ (progenitor masses $M_{\text{ZAMS}} \lesssim 1 M_{\odot}$). Hence, our calculations demonstrate that, contrary to the accepted paradigm, stable nuclear burning in *low-mass*, low-metallicity white dwarfs can be the main energy source, delaying substantially their cooling times at low luminosities.

4. SUMMARY AND CONCLUSIONS

We have computed a set of cooling sequences for hydrogen-rich white dwarfs with very low metallicity progenitors, which are appropriate for precision white dwarf cosmochronology of old stellar systems. Our evolutionary sequences have been self-consistently evolved through all the stellar phases. That is, we have computed the evolution of the progenitors of white dwarfs from the ZAMS, through the core hydrogen- and helium-burning phases to the TP-AGB phase. Finally, we have used

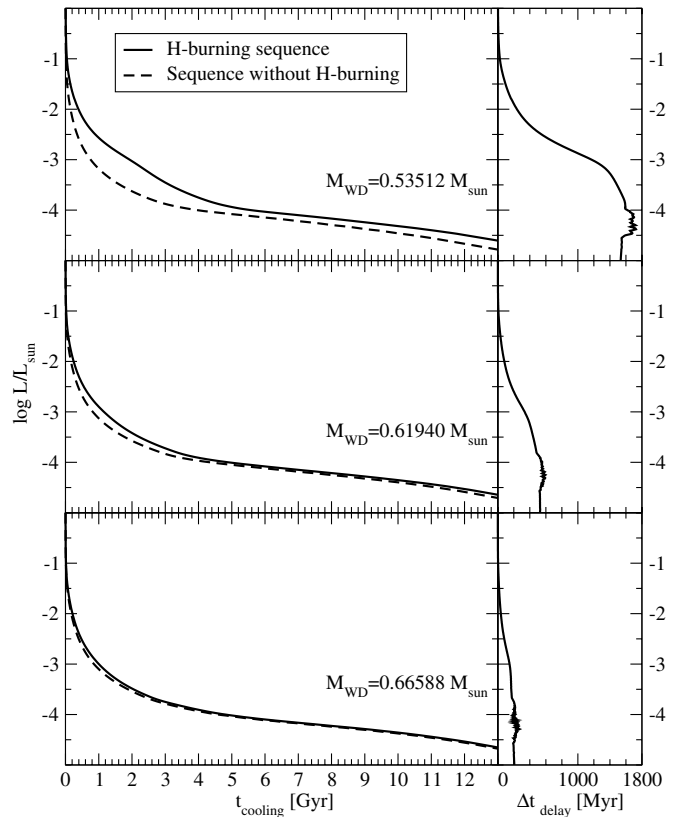


Figure 3. Impact of the nuclear burning on the cooling time of representative $Z = 0.0001$ white dwarf sequences. Note that between $\log(L/L_{\odot}) = -2$ and $\log(L/L_{\odot}) = -4$, disregarding the energy released by nuclear burning underestimates the cooling times by more than a factor of two.

these self-consistent models to compute white dwarf cooling tracks. To the best of our knowledge, this is the first set of fully evolutionary calculations of low-metallicity progenitors resulting in white dwarfs cooling tracks covering the relevant range of initial main sequence and, correspondingly, white dwarf masses. We emphasize that our complete evolutionary calculations of the history of the progenitors of white dwarfs allowed us to have self-consistent white dwarf initial models. Specifically, in our calculations the masses of the hydrogen-rich envelopes and of the helium shells beneath them were obtained from evolutionary calculations, instead of using typical values and artificial initial white dwarf models. We have shown that this has implications for the cooling of low-mass white dwarfs resulting from low-metallicity progenitors, as the masses of these layers not only control the cooling speed of these white dwarfs, but also determine if they are able to sustain residual nuclear burning. Specifically, our calculations show that the masses of the envelopes of the resulting white dwarfs are more massive than those of their solar metallicity counterparts. These white dwarfs having more massive envelopes, the role of nuclear energy release becomes more prominent and the white dwarf cooling times for the same luminosity turn out to be considerably larger than those of white dwarfs descending from progenitors with larger metallicity. In particular, we found that for $Z = 0.0001$, and for white dwarf masses smaller than about $0.6 M_{\odot}$, the nuclear energy release is the main energy source contributing to the stellar luminosity until luminosities as low as $\log(L/L_{\odot}) \simeq -3.2$ are reached.

Since very low metallicity stars are expected to be members of the galactic halo or very old globular clusters, our findings could

have consequences not only for the determination of the ages of low-mass white dwarfs, but also may have a noticeable effect on the shape of their white dwarf luminosity functions. However, we expect that the impact of residual nuclear burning on the age determinations of such low-metallicity populations should be modest, of the order of $\sim 5\%$. Nevertheless, this finding questions the correctness of using standard white dwarf cooling sequences in which no nuclear burning is considered, or which oversimplify the previous evolutionary history of the progenitor star, to date individual low-mass white dwarfs—those with masses $\lesssim 0.6 M_{\odot}$ —belonging to low-metallicity populations. However, the detailed study of how quiescent nuclear burning affects the shape of the white dwarf luminosity function of old populations is out of the scope of the present Letter and will be explored in forthcoming works.

Part of this work was supported by AGENCIA through the Programa de Modernización Tecnológica BID 1728/OC-AR, by PIP 112-200801-00940 grant from CONICET, by MCINN grant AYA2011-23102, by the ESF EUROCORES Program EuroGENESIS (MICINN grant EUI2009-04170), by the European Union FEDER funds, and by the AGAUR.

REFERENCES

- Althaus, L. G., Córscico, A. H., Bischoff-Kim, A., et al. 2010a, *ApJ*, **717**, 897
 Althaus, L. G., Córscico, A. H., Isern, J., & García-Berro, E. 2010b, *A&ARv*, **18**, 471
 Althaus, L. G., García-Berro, E., Isern, J., Córscico, A. H., & Miller Bertolami, M. M. 2012, *A&A*, **537**, A33
 Althaus, L. G., García-Berro, E., Renedo, I., et al. 2010c, *ApJ*, **719**, 612
 Althaus, L. G., Serenelli, A. M., Córscico, A. H., & Montgomery, M. H. 2003, *A&A*, **404**, 593
 Althaus, L. G., Serenelli, A. M., Panei, J. A., et al. 2005, *A&A*, **435**, 631
 Angulo, C., Arnould, M., Rayet, M., et al. 1999, *NuPhA*, **656**, 3
 Bono, G., Salaris, M., & Gilmozzi, R. 2013, *A&A*, **549**, A102
 Cassisi, S., Potekhin, A. Y., Pietrinferni, A., Catelan, M., & Salaris, M. 2007, *ApJ*, **661**, 1094
 Córscico, A. H., Althaus, L. G., García-Berro, E., & Romero, A. D. 2013, *JCAP*, **6**, 32
 Córscico, A. H., Althaus, L. G., Miller Bertolami, M. M., et al. 2012a, *MNRAS*, **424**, 2792
 Córscico, A. H., Althaus, L. G., Romero, A. D., et al. 2012b, *JCAP*, **12**, 10
 Ferguson, J. W., Alexander, D. R., Allard, F., et al. 2005, *ApJ*, **623**, 585
 Fontaine, G., & Brassard, P. 2008, *PASP*, **120**, 1043
 García-Berro, E., Hernanz, M., Isern, J., & Mochkovitch, R. 1995, *MNRAS*, **277**, 801
 García-Berro, E., Lorén-Aguilar, P., Torres, S., Althaus, L. G., & Isern, J. 2011, *JCAP*, **5**, 21
 García-Berro, E., Torres, S., Althaus, L. G., et al. 2010, *Natur*, **465**, 194
 Graboske, H. C., Dewitt, H. E., Grossman, A. S., & Cooper, M. S. 1973, *ApJ*, **181**, 457
 Groenewegen, M. A. T., Sloan, G. C., Soszyński, I., & Petersen, E. A. 2009, *A&A*, **506**, 1277
 Hansen, B. M. S., Anderson, J., Brewer, J., et al. 2007, *ApJ*, **671**, 380
 Horowitz, C. J., Schneider, A. S., & Berry, D. K. 2010, *PhRvL*, **104**, 231101
 Iben, I., Jr., & MacDonald, J. 1986, *ApJ*, **301**, 164
 Iglesias, C. A., & Rogers, F. J. 1996, *ApJ*, **464**, 943
 Isern, J., García-Berro, E., Hernanz, M., & Chabrier, G. 2000, *ApJ*, **528**, 397
 Isern, J., García-Berro, E., Torres, S., & Catalán, S. 2008, *ApJL*, **682**, L109
 Isern, J., Mochkovitch, R., García-Berro, E., & Hernanz, M. 1997, *ApJ*, **485**, 308
 Miller Bertolami, M. M., Althaus, L. G., Olano, C., & Jiménez, N. 2011, *MNRAS*, **415**, 1396
 Renedo, I., Althaus, L. G., Miller Bertolami, M. M., et al. 2010, *ApJ*, **717**, 183
 Rohrmann, R. D., Althaus, L. G., García-Berro, E., Córscico, A. H., & Miller Bertolami, M. M. 2012, *A&A*, **546**, A119
 Salaris, M., Althaus, L. G., & García-Berro, E. 2013, *A&A*, **555**, A96
 Salaris, M., Cassisi, S., Pietrinferni, A., Kowalski, P. M., & Isern, J. 2010, *ApJ*, **716**, 1241
 Schröder, K.-P., & Cuntz, M. 2005, *ApJL*, **630**, L73
 Weiss, A., & Ferguson, J. W. 2009, *A&A*, **508**, 1343
 Winget, D. E., & Kepler, S. O. 2008, *ARA&A*, **46**, 157
 Winget, D. E., Kepler, S. O., Campos, F., et al. 2009, *ApJL*, **693**, L6
 Winget, D. E., Sullivan, D. J., Metcalfe, T. S., Kawaler, S. D., & Montgomery, M. H. 2004, *ApJL*, **602**, L109